Supporting Information

Title: Ab-initio study of short-range ordering in vanadium-based disordered rocksalt structures

Authors: Zinab Jadidi[1,2], Julia H. Yang[1,2], Tina Chen[1,2], Luis Barroso-Luque[1,2], Gerbrand Ceder[1,2]

[1] Department of Materials Science and Engineering, Berkeley CA 94720

[2] Materials Sciences Division, Lawrence Berkeley National Laboratory, Berkeley CA 94720

Corresponding author: gceder@berkeley.edu

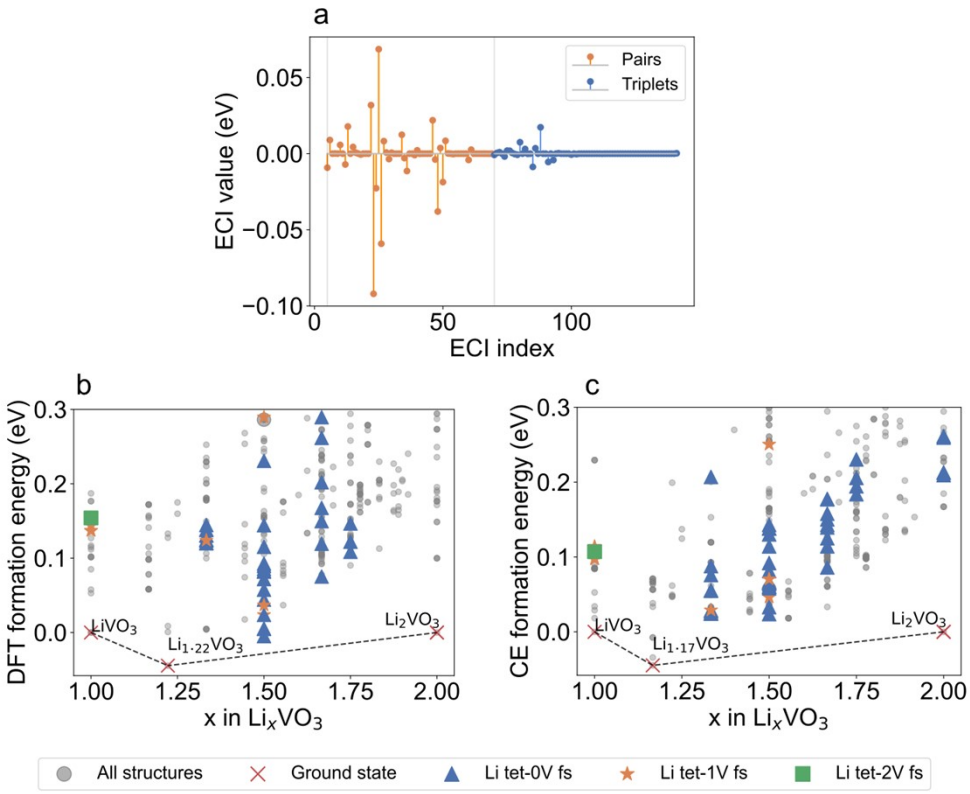

Figure S1: (a) ECI value vs. ECI index. Each ECI index corresponds to a specific decoration of Li^{+}, V^{4+}, and V^{5+} in pair (orange) and triplet (blue) clusters. **(b)** DFT convex hull showing the energies of structures with an energy above the hull below 0.3 eV. The DFT formation energies of all the structures are marked with gray circles. The ground states (Li_2VO_3, $LiVO_3$, and $Li_{1.22}VO_3$) are marked by red crosses. Structures that contain tetrahedral Li with 0, 1, and 2 face-sharing V are marked by blue triangles, orange stars, and green squares, respectively. It is apparent that up to 2 Li tet-V face-sharing is possible based on the DFT data. **(c)** CE convex hull. The ground states (Li_2VO_3, $LiVO_3$, and $Li_{1.17}VO_3$) are marked by red crosses. Although the ground states $LiVO_3$ and Li_2VO_3 are the same in both the DFT and CE convex hulls, there is a discrepancy between the DFT and CE convex hull in predicting the ground state for $Li_{1.22}VO_3$. DFT predicts $Li_{1.22}VO_3$ as the ground state, but it is not predicted in the CE convex hull, where

$Li_{1.17}VO_3$ is favored instead. Similar discrepancies in preserving the ground states have been observed in cluster expansions of other high-component systems. (1,2)

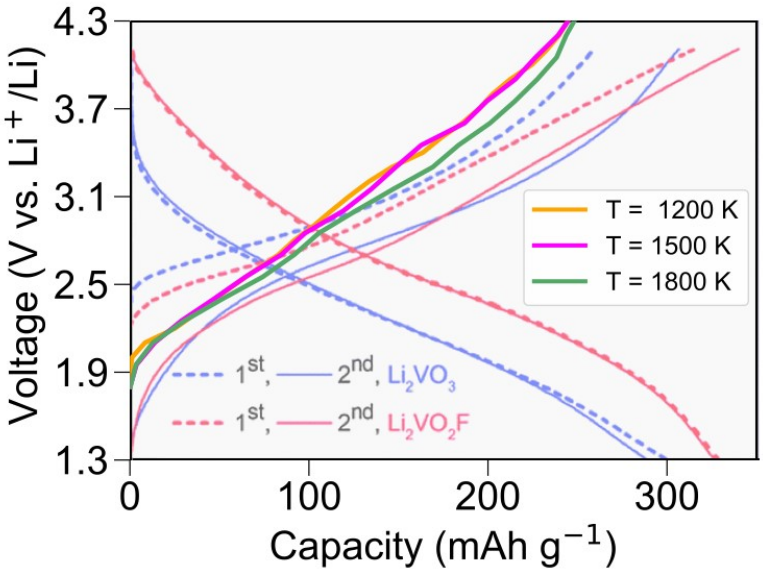

Figure S2: Comparison between the experimental Li_2VO_3 voltage profile obtained by Chen et al. in the dotted blue curve (3) with our SGC MC calculated ones in the Li/V framework sampled at T = 1200 K, 1500 K, and 1800 K. The voltage profile obtained at the simulated temperature of 1800 K shows greater similarity to the experimental voltage profile (dotted blue curves) obtained by Chen et al. (3), specifically at higher delithiated states.

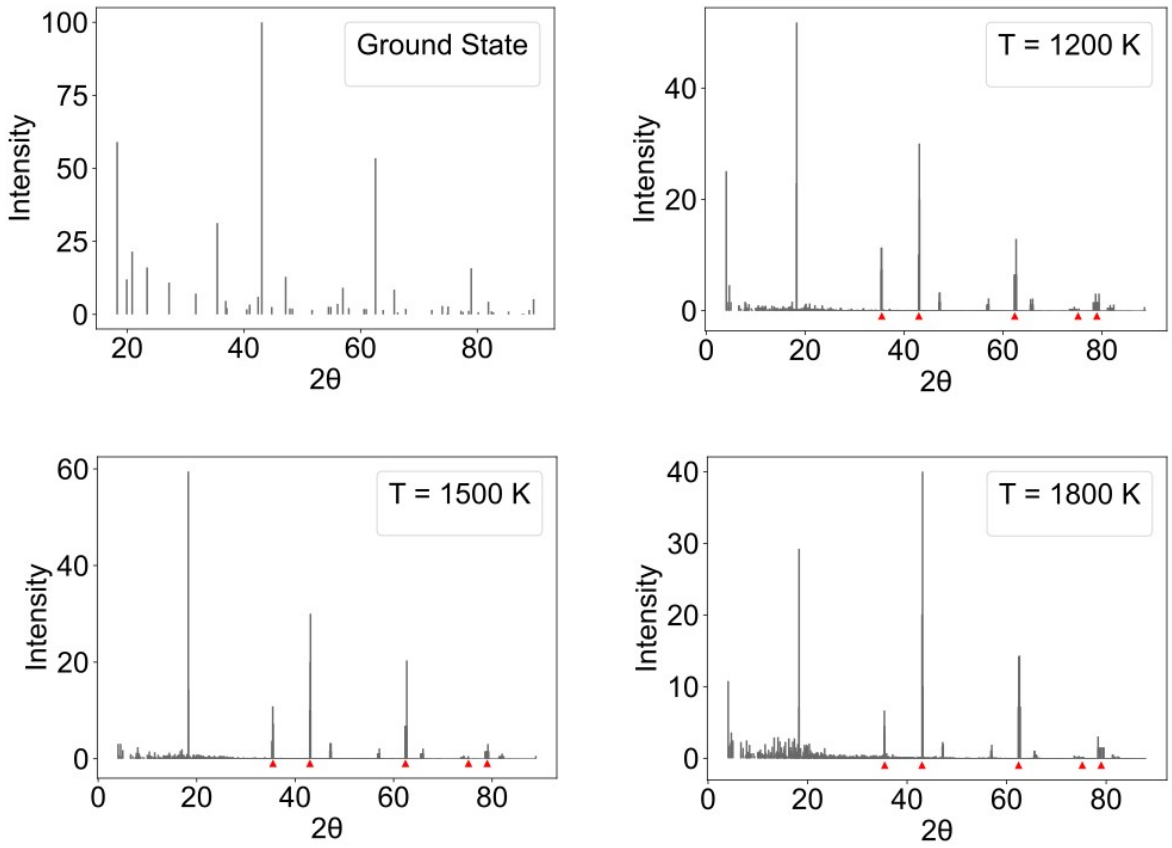

Figure S3: Simulated XRD pattern of fully lithiated Li_2VO_3 in 9×8×9 supercell using pymatgen python package. (4) At the ground state, the XRD pattern corresponds to that of the semi-layered ground state of Li_2VO_3. The simulated XRD patterns for T = 1200, 1500, and 1800 K are averaged over 10 Li/V^{4+} sampled configurations. The main rocksalt peaks (at 38°,43°,63°,76°, and 80°) are marked with red triangles in all cases. While there are peaks at angles below 20 degrees in all three cases, the intensities of the low-angle peaks at 1200 and 1500 K are higher than the main peak at 43°. This, however, does not apply to the Li/V^{4+} configurations sampled at 1800 K.

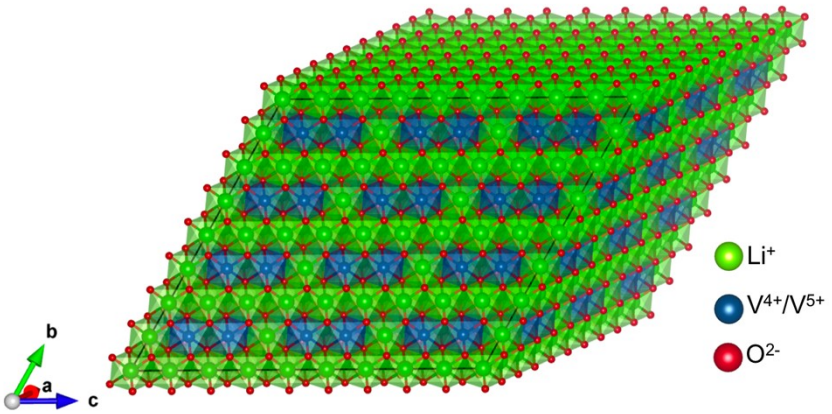

Figure S4: Schematic of fully lithiated Li_2VO_3 at its ground state, which consists of alternating Li^+ and Li^+/V^{4+} layers.

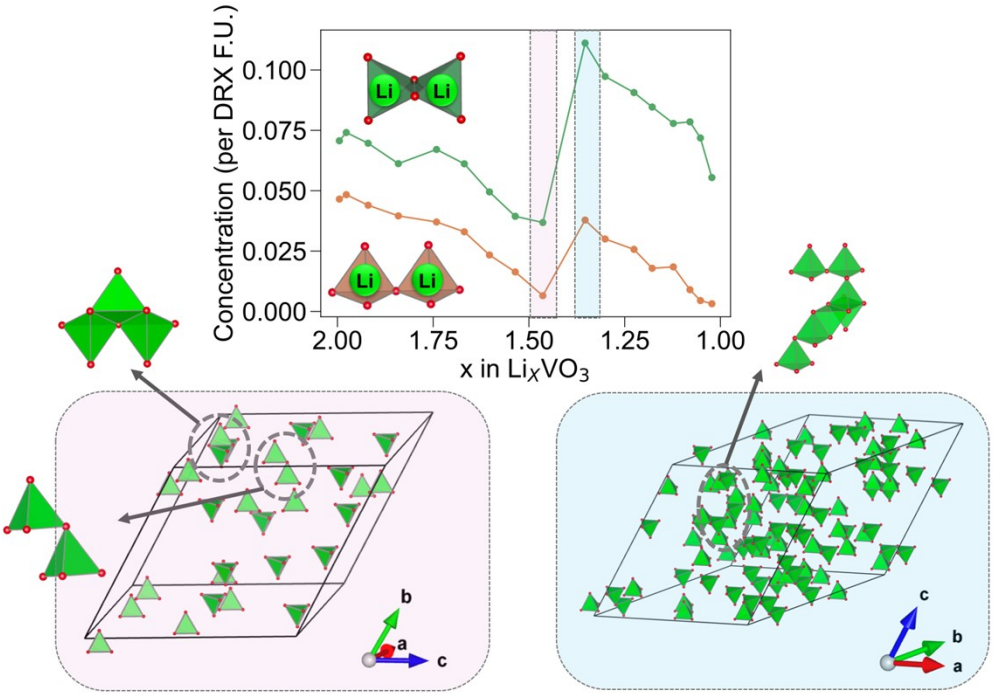

Figure S5: Concentration of edge-sharing (depicted in green) and corner-sharing (represented in orange) Li-tetrahedra as a function of Li content in Li_xVO_3. In our system, the composition ~ $Li_{1.35}VO_3$, highlighted in light blue, exhibits the highest concentration of tetrahedral Li, while the composition ~ $Li_{1.44}VO_3$, highlighted in light pink, shows the lowest concentration of tetrahedral

Li. These two cases are further visualized in the bottom figures, which display only the tetrahedral sites. The bottom left figure shows a schematic of Li tetrahedra in ~ $Li_{1.44}VO_3$, where most tetrahedral Li are not edge-sharing or corner-sharing with other tetrahedral Li. By further delithiation of $Li_{1.44}VO_3$, more tetrahedral sites become available for Li to occupy, resulting in clusters of tetrahedral Li in the ~ $Li_{1.35}VO_3$.

Note 1: Challenges of the CE of the high-component system $Li_{2-x}VO_3$, $0 < x < 1$

This study is based on a lattice cluster expansion of high-component systems with quaternary disorder (considering $Li^+/V^{4+}/V^{5+}$ and vacancies) on octahedral sites and binary disorder (Li^+ and vacancies) on tetrahedral sites. The fitting of the ECI for this cluster expansion uses an approach applied in other high-component systems. (1,2,5) In this study, we find there are several challenges associated with structural mapping and sampling when addressing the Li–Vac–V–O system in particular.

First, the V^{5+} octahedron experiences significant distortion in part because it is a d_0 element that can strongly distort without an energetic penalty. (6,7) As another example, the presence of vacancies in the system can allow for nearby cations to relax towards the vacancy and reduce electrostatic repulsion from its nearby cations. These distortions make the mapping of the relaxed structure to the lattice-site representation of the cluster expansion extremely challenging as the anion framework becomes highly distorted.

Second, the addition of the interstitial tetrahedral site to the cluster expansion increases the size of the configurational space significantly, and many configurations that could technically exist are practically not achievable. For instance, face-sharing metal-rich clusters have very strong electrostatic repulsion that makes the local configuration unstable. When these

configurations are dynamically unstable, they relax away in DFT. As a result, our training data may contain insufficient sampling containing these types of local configurations. We find that this lack of sampling makes the Monte Carlo equilibration more difficult because equilibration may sample structures outside our training set. The dearth of training data with these types of face-sharing configurations may cause our model to represent the energies of structures with face-sharing less accurately and may be a reason for the 2 V– and 3 V–Li tet face-sharing in some of the simulations. Having these face-sharing features as well as the *possibly* larger number of tetrahedral sites compared to the experimental material could be two reasons why the simulated voltage profile is sloppier than the experimental one. Note that metal–Li tet face-sharing features have also been theoretically observed in other studies. (1,5,8)

References

1. Chen T, Yang J, Barroso-Luque L, Ceder G. Removing the Two-Phase Transition in Spinel LiMn2O4 through Cation Disorder. ACS Energy Lett. 2022 Dec 2;314–9.

2. Yang JH, Chen T, Barroso-Luque L, Jadidi Z, Ceder G. Approaches for handling high-dimensional cluster expansions of ionic systems. Npj Comput Mater. 2022 Dec;8(1):133.

3. Chen R, Ren S, Yavuz M, Guda AA, Shapovalov V, Witter R, et al. Li+ intercalation in isostructural Li2VO3 and Li2VO2F with O2− and mixed O2−/F− anions. Phys Chem Chem Phys. 2015 Jun 24;17(26):17288–95.

4. Ong SP, Richards WD, Jain A, Hautier G, Kocher M, Cholia S, et al. Python Materials Genomics (pymatgen): A robust, open-source python library for materials analysis. Comput Mater Sci. 2013;68:314–9.

5. Yang JH, Ceder G. Activated Internetwork Pathways in Partially-Disordered Spinel Cathode Materials with Ultrahigh Rate Performance. Adv Energy Mater. 2023;13(4):2202955.

6. Ok KM, Halasyamani PS, Casanova D, Llunell M, Alemany P, Alvarez S. Distortions in Octahedrally Coordinated d ^{0} Transition Metal Oxides: A Continuous Symmetry Measures Approach. Chem Mater. 2006 Jul 1;18(14):3176–83.

7. Urban A, Abdellahi A, Dacek S, Artrith N, Ceder G. Electronic-structure origin of cation disorder in transition-metal oxides. Phys Rev Lett. 2017;119(17):176402.

8. Guo X, Chen C, Ong SP. Intercalation Chemistry of the Disordered Rocksalt Li3V2O5 Anode from Cluster Expansions and Machine Learning Interatomic Potentials. Chem Mater. 2023;35(4):1537–46.